OF

N81-13412

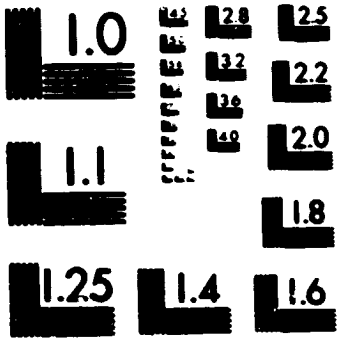

MICROCOPY RESOLUTION TEST CHART
NATIONAL BUREAU OF STANDARDS 1963-A

NASA

Technical Memorandum 81988

APPLICATION OF DIGITAL TERRAIN DATA TO QUANTIFY AND REDUCE THE TOPOGRAPHIC EFFECT ON LANDSAT DATA

C. O. Justice, S. W. Wharton and B. N. Holben

AUGUST 1980

National Aeronautics and Space Administration

Goddard Space Flight Center
Greenbelt, Maryland 20771

TM 81988

APPLICATION OF DIGITAL TERRAIN DATA TO QUANTIFY AND REDUCE THE TOPOGRAPHIC EFFECT ON LANDSAT DATA

C. O. JUSTICE*
S. W. WHARTON
B. N. HOLBEN
Earth Resources Branch (Code 923)
NASA/GSFC
Greenbelt, MD 20771
USA

August 1980

*C. Justice is an NRC Resident Research Associate at NASA/GSFC

APPLICATION OF DIGITAL TERRAIN DATA TO QUANTIFY AND REDUCE THE TOPOGRAPHIC EFFECT ON LANDSAT DATA

1. Introduction

The topographic effect is defined as the variation in radiances from inclined surfaces compared to radiance from a horizontal surface as a function of the orientation of the surfaces relative to the light source and sensor position (Holben and Justice 1980). On Landsat images of rugged terrain, this effect is manifested by the visual impression of relief (figure 1). Holben and Justice (1979) measured the topographic effect on remotely sensed data and showed the effect to be most extreme at low solar elevations and greatest for slopes in the principal plane of the sun. They also showed by a Landsat simulation study that the topographic effect can produce a considerable variation in radiances associated with a given cover type and may lead to poor cover-classification results. Sadowski and Malila (1977) demonstrated that reflectances vary as a function of slope and aspect and that such terrain variations complicate the task of discriminating woodland categories with remotely sensed data. Several other studies have demonstrated the need to consider topographic variations when undertaking Landsat cover classification for areas of mountainous terrain (Hoffer and Staff 1975, Anuta 1976, Miller *et al.* 1978, Strahler *et al.* 1978, Hoffer *et al.* 1979, Strahler *et al.* 1979, Williams and Miller 1979).

The above studies incorporated elevation data with Landsat data to improve cover classification accuracies. Removal or reduction of the topographic effect before classification will reduce the variation associated with the radiance for a given cover type and thereby increase the likelihood of class separability. Sadowski and Malila (1977) showed that changes in reflectance resulting from different topographic location resulted in spectral overlap of forested and nonforested sites. Williams *et al.* (1979) demonstrated that the utility of Landsat data for mapping gypsy moth defoliation of forest canopies in the mountains of central Pennsylvania was severely restricted by topographic variations. This restriction was most pronounced in separating levels of defoliation on slopes of different orientations.

The objective of this study is to quantify and reduce the topographic effect found in Landsat data for an area adjacent to that examined by Williams *et al.* (1979) in central Pennsylvania. The next section of the paper describes the field area selected for this study and the methods and data base used in the analysis. The third section discusses four techniques for reducing the topographic effect. The fourth section examines the strength of topographic effect in the data and the effectiveness of the four techniques for reducing the effect. The fifth section summarizes the results of the analysis and discusses the implications of the results.

2. Description of study area, data base, and methods

The study area is located in Perry County, north of Harrisburg, in central Pennsylvania and is contained within the 7.5-minute Reward quadrangle (figure 1). The ridge and valley topography of the area, formed from a series of eroded anticlines and synclines, is composed of Ordovician limestones, sandstones, and shales, running northeast to southwest across the area. Buffalo Mountain, the ridge examined in this study, runs linearly northeast to southwest, with a maximum height of 409 m. The ridge was chosen for its constant slopes and aspects and uniform forest cover. Block diagrams created from the digital terrain data show the topography of the study area (figures 2 and 3). Buffalo Mountain has three major slope units: moderate (*ca* 9°) and steep (*ca* 22°) rectilinear slopes of northwest aspect and moderate (c. 15°) slopes of southeast aspect. The ridge is covered by a mixed deciduous oak woodland consisting predominantly of white oak, red oak, chestnut oak, and black oak. A field visit to the study area revealed complete crown closure throughout the study area and minimum differences in the cover type, distribution, and density between the two predominant aspects.

Two types of data were integrated to provide the data base used in this study; namely, Landsat multispectral scanner (MSS) data and digital terrain data. The image-processing system used for this study was the IDIMS (Interactive Digital Image Manipulation System) produced by E.S.L. (Electromagnetic System Laboratory) Inc; the particular installation is at NASA/Goddard Space

Flight Center (GSFC), Greenbelt, MD, USA. It is comprised of a Hewlett-Packard 3000 mini-computer with a programmable array processor and specific software for image analysis. The various data planes used in the study were created as image files on the IDIMS system.

The Landsat data chosen for this study were for July 19, 1976, with a solar elevation of 55°. This high-sun-angle image was selected because it depicts the period of maximum foliage, which enables optimum discrimination (Williams *et al.* 1979). Furthermore, it depicts a time close to the summer solstice, when the topographic effect is at a minimum (Holben and Justice 1979), and is most likely, therefore, to be chosen for analysis of cover types. From the raw Landsat data the MSS 7/5 and 6/5 band-ratio images were created. For ease of integration the Landsat data were resampled to 50 m and registered to the 1:24,000 topographic sheet.

The digital terrain data used in this study were the 30-m Digital Elevation Model (DEM) data obtained from the U.S. Geological Survey (USGS) Digital Applications Team, Reston, Virginia (figure 4). The DEM data should be distinguished from the 200-foot Defense Mapping Agency data, also available from the USGS. The coarser resolution of the latter has been criticized with reference to the usefulness of the horizontal resolution and the height accuracy (Stow and Estes 1979). The DEM data are derived from orthophotos and are available for selected 7.5-minute quadrangles within the USA (McEwen and Elassal 1978).

The height accuracy of the DEM data was evaluated by comparing 91 elevation control points on the topographic map with the corresponding height values for the same locations from the terrain data before the data resampling. The average deviation of the DEM height values from the corresponding topographic map values was 5.92 m. Further examination of the best matching point within a 3 × 3 window of the DEM data reduced the average variation to 2.79 m. The DEM data were well within the 7-m height accuracy claimed by the USGS (Elassal 1980). From the 50-m resampled DEM elevation data, both slope (figure 5a) and aspect (figure 5b) were calculated for each elevation point, by use of a four-cell elevation matrix, by applying a modification

of an algorithm developed by Sharpnack and Akin (1969). Software was developed to use slope, aspect, solar elevation, and azimuth to calculate the incidence angle for each pixel (figure 5c). The Landsat data were registered to the 7.5-minute topographic map for the Reward Quadrangle and the eight surrounding map quadrangles. Eighty-four evenly dispersed control points were chosen for the map sheets and the Landsat data. The root mean square (rms) error was 0.79 pixels, and the maximum error was 1.75 pixels. The five control points located within the Reward Quadrangle had a rms of 0.73 pixels, with a maximum error of 1.03 pixels.

3. Techniques examined for reducing the topographic effect

Four techniques for reducing the topographic effect are examined in this study, namely, spectral-band ratioing and application of a Lambertian model, a modified Lambertian model, and a non-Lambertian model.

Spectral-band ratioing in its simplest form consists of dividing the radiance values in one channel by the corresponding radiance values in a second channel. Ratioing has been proposed as a way of reducing multiplicative effects within multispectral data, e.g., by Kriegler *et al.* (1969), Crane (1971), and Vincent (1973). The topographic effect of direct light is one such multiplicative effect. A detailed account of band ratioing as a technique for reducing the topographic effect on ground-based radiometer data is presented by Holben and Justice (1980), who showed that ratioing reduced the topographic effect on their data by an average of 83 per cent. However, a study by Williams *et al.* (1979) on Landsat data of central Pennsylvania showed the spectral-band ratioing did not remove slope- and aspect-induced variations to enable improved classification.

The second technique examined was the application of a Lambertian reflectance model. This model is described by Justice and Holben (1979) and is based on the assumption that the surface being sensed is Lambertian. A Lambertian surface is one that scatters light equally in all directions. The radiance from the surface can therefore be modelled by the cosine of the incidence angle, where the incidence angle is the angle between the surface normal and the solar beam (Robinson 1965).

Lambertian Model: $L = Ln (\cos i)$,

where L=radiance,

Ln=normalized radiance,

i=incidence angle.

The Lambertian model assumes the reflected light to be directly proportional to the incident light. The relationship between data derived with the Lambertian model and radiances received by ground-based sensors was examined by Holben and Justice (1979), there was a strong statistical relationship between the data sets. The Lambertian model has been examined for correcting sun angle and topographic effects in Landsat data (Cicone *et al.* 1977, Justice 1978, Hoffer *et al.* 1979, Tom *et al.* 1979, Smith *et al.* 1980, Strahler *et al.* 1979). Hoffer *et al.* (1979) applied the Lambertian model to Landsat data and found that this correction slightly decreased classification accuracy for a range of forest cover types. Smith *et al.* (1980) found that the Lambertian assumption was only valid over a small range of incidence angles for pine-forest cover types. Cicone *et al.* (1977) found high statistical correlations between Landsat radiances and incidence angle, but found that the Lambertial model overcorrected the data. To compensate for this overcorrection, Cicone *et al.* (1977) modified the Lambertian assumption by multiplying the slope angle by the solar zenith angle and then calculating the incidence angle. This modification was determined empirically with data for two solar elevations, and it led to improvements over the Lambertian model.

All natural surfaces have preferred orientations of scattering (Kriebel 1976, 1978), and thus they are more satisfactorily modelled by a non-Lambertian model. Smith *et al.* (1980) applied a non-Lambertian model to Landsat data, using a function developed by Minnaert (1941, 1961). The model takes into consideration the incidence angle and the exitance angle made with the surface, as a function of K, a constant value.

Non-Lambertian Model: $L=Ln\ (\cos^{K}i)\ (\cos^{K-1}e)$,

where: L=radiance,

Ln=radiance when i=e=0,

i=incidence,

e=exitance,

K=Minnaert constant.

The K value is derived from the data and is equivalent to the slope of the regression line formed by plotting log ((L)(cos e)) against log ((cos i)(cos e)). The K value gives a measure of the Lambertianess of a surface. a K of 1 signifies a Lambertian surface. Most natural surfaces have values between 0 and 1. Smith *et al.* (1980) showed that the non-Lambertian model performed significantly better than the Lambertian model in reducing terrain-induced variations on pine woodland. Justice and Holben (1979) examined the Minnaert function with reference to ground-based data and found a similar improvement over the Lambertian model for reducing the topographic effect. However, subsequent theoretical examination of the K value by the authors has shown that the model is inappropriate for K values of greater than 1, i.e., in cases in which there is a high spectual component.

4 Analysis

The analysis of the data is subdivided into four major sections. The first section describes the measurement of the topographic effect for the Landsat data taken at 55° solar elevation by examination of randomly selected test sites. The second section presents a detailed analysis of the topographic effect for six sample transects taken across the mountain ridge. The third section examines the variability of the Landsat radiance data for the six transects, after the application of spectral-band ratioing and the Lambertian and non-Lambertian normalization models to reduce the topographic effect. The final section includes application of the optimum normalization procedure to the Landsat data and a comparison of the corrected and the uncorrected radiance data.

4.1. The topographic effect on selected test sites

The Landsat data of the Reward Quandrangle for MSS 7 (0.8-1.1 μm) (figure 6) show the topographic effect on Buffalo Mountain ridge, which runs northeast-southwest across the image. The deciduous woodland canopy has a high reflectance in the infrared for both dominant aspects, but the northwest slope of the ridge facing away from the sun is visibly darker than the southeast slope. The MSS 4 and 5 (figure 7)(0.5-0.6 μm and 0.6-0.7 μm) show no visible topographic effect, because of the low reflectivity of the woodland canopy in these two channels, allowing the atmospheric path radiance to dominate. The major variation that can be seen on the mountain ridge in channels 4 and 5 is caused by sensor banding. This is probably because at low reflectances the topographic effect, although present, is obscured by the quantization of the MSS sensor system (Holben and Justice, 1980). The MSS 6 (0.7-0.8 μm) image was visually similar to that of MSS 7.

For demonstration of the topographic effect on the Landsat data, three type sites were chosen to represent the major slope-aspect combinations on Buffalo Mountain, namely, southeast aspect and moderate slope, northwest aspect and moderate slope, and northwest aspect and steep slope. Test sites were randomly selected for each of the three locations along the mountain ridge. Four sites totaling 767 pixels were selected for the southeast aspect location. Four sites totaling 660 pixels and five sites totaling 213 pixels were selected for the northwest aspect moderate- and steep-slope sites, respectively. The number of pixels in the latter class was restricted by the extent of the slope class. Mean solar incidence angles of 44.5°, 61.7°, and 73.5° were calculated for the southeast-aspect moderate slopes, northwest-aspect moderate slopes, and northwest-aspect steep slopes. Calculation of mean pixel values for each test site revealed distinct grouping in MSS 6 and 7 with respect to aspect (figure 8).

Field checking of the sites before the analysis had shown no observable differences in the woodland cover for the three locations. The differences in the mean pixel values were therefor associated primarily with the topographic variation. The highest mean pixel values associated with the oak woodland cover were in MSS 6 for the southeast aspect. However, the highest individual

radiances were for MSS 7, which was quantized to 64 levels, half the quantization level of the other three channels. The northwest-aspect moderate-slope radiances for MSS 6 and MSS 7 were higher than the steep-slope radiances for the same aspect. Three distinct ranges of mean pixel values were obtained for the three slope-aspect classes for MSS 6 and 7. For MSS 6 a difference of 17 pixel values separated the mean values for the sites associated with the southeast and northwest aspects. Such a large range indicates that selection of training sites for cover classification from one slope-aspect location may not adequately describe the radiances from the same cover from other locations. The degree to which this may affect the classification results depends largely on the location and distribution of other cover-class radiances within the classification-feature space.

4.2 Analysis of sample transects

Six sample transects of Landsat data across the mountain ridge were taken to examine the topographic effect in detail and to assess the statistical relationship between the Landsat radiances and the data derived with the proposed models. Each transect contained 20 pixels of Landsat data. The mean pixel value, standard deviation, and range were calculated for each transect (table 1). Examination of these values shows the uniformity of Landsat radiances between the different transects. In MSS 6, Transect 3 had the greatest range, 21 pixel values, and in MSS 7, Transect 6 had the greatest range, 14 pixel values. Elevation, pixel values, and incidence angles for a sample transect are presented in figure 9. There is a negative relationship between pixel value and incidence angle; the lowest pixel values were associated with the highest incidence angles and vice versa.

The statistical relationship between the radiances and the data derived from the models was assessed for each transect with Pearson's product-moment correlation coefficient (table 2). The correlation coefficient gives an indication of the strength of the linear relationship between two variables. Correlation coefficients (r) were insignificant at the 0.05 level for MSS 4 and 5 for all three models. Strong positive relationships ($r \geq 0.84$) were found for data derived with the Lambertian and non-Lambertian models, and a strong negative relationship was found for data derived

with the modified Lambertian model for all transects. There was no substantial difference in the size of the r values among the three models.

4.3 Evaluation of topographic effect reduction techniques

Spectral-band ratioing and the three models were assessed for reducing the topographic effect on Pennsylvania Landsat data.

Coefficients of variation (CVs) were calculated for the ratios of MSS 6/5 and MSS 7/5 for each transect and are presented for comparison with CVs for the raw data (table 3). The CV is the standard deviation divided by the mean value, and it is used to compare variations within data sets. In this study a decrease in topographic effect is signified by a decrease in the CV. The CVs indicated a greater variation in the MSS 7/5 ratio than in the MSS 6/5 ratio, because of the higher variation in MSS 7. The CVs for MSS 6/5 and 7/5 ratios decreased slightly from the CVs for the raw MSS data for three out of six transects. The poor reduction in the topographic effect by the MSS 6/5 and 7/5 ratios is due to the negligible variation in MSS 5. The relatively constant radiance in MSS 4 and MSS 5 is associated with the high absorption by the green leaves of the deciduous woodland and means that ratioing is effectively dividing MSS 7 and MSS 6 by a constant value.

Application of the Lambertian model to the data to reduce the topographic effect (i.e., division of each pixel by cos i) led to a large increase in the CV for each transect over the variation for the raw data (table 3). Dividing the radiance from a Lambertian surface by cos i normalizes the radiance to the equivalent radiance from a flat surface with the sun overhead. This increase in the CVs is presumably due to the inapplicability of the Lambertian assumption for the woodland cover type in question. The largest CV was found for normalized MSS 4 and 5 data, probably because of the very small proportion of the MSS 4 and 5 radiance that was directly related to the variation in the incidence angle, i.e., direct light reflectance. Over the majority of slopes, the

diffuse-light component appears essentially constant (Justice and Holben, 1980). The modified Lambertian model developed by Cicone *et al.* (1977) was a considerable improvement over the Lambertian model in reducing the topographic effect (table 3), but for all transects, it increased the topography-induced variation above that found in the raw Landsat data.

Application of the non-Lambertian model to the transect data involved calculation of the Minnaert K values for each transect (table 4). The regression lines used to calculate the K values for MSS 4 and 5 had r^2 values of less than 0.50 and were deemed invalid for any correction of the data. The low r^2 values were a direct result of the negligible variation in the MSS 4 and 5 radiances. The regression lines used to derive the K values for MSS 6 and 7 had $r^2 \geq 0.74$, with K values ranging from 0.26 to 0.37 for MSS 7 and 0.20 to 0.32 for MSS 6. The r^2 values for these data were higher than those reported by Smith *et al.* (1980) and were less variable within the cover type. The values were then substituted in the non-Lambertian model $[(\cos^{K}i)(\cos^{K-1}e)]$ for each transect, and the CVs were calculated for the corrected data (table 3). The CVs for the non-Lambertian model were markedly smaller than the CVs for raw MSS 6 and 7 data. The maximum reduction in the CVs was from 10.5 to 3.9 for MSS 6 and from 15.0 to 4.0 for MSS 7.

4.4 Application and Assessment of the non-Lambertian model to correct the Landsat data

The non-Lambertian model was shown to be the best correction procedure for reducing the topographic effect (table 3). Before applying the non-Lambertian model to the Landsat data for Buffalo Mountain, it was necessary to decide which K value to substitute into the model. Use of the model with multiple K values would be too complex for any operational study. Therefore a sensitivity test was undertaken to assess how application of a single K value to all the transects for MSS 6 would effect the CV values. Coefficients of variation were calculated for each transect with data derived from the non-Lambertian model and K values from 0 to 1 (table 5). Table 5 shows considerable variation in CV for each transect over a range of K values. A mean K value of 0.269 was selected from the transect study and applied to the data. This mean K value led to a

negligible change in the CV value from those derived with individual K values from each transect. The non-Lambertian model with a K value of 0.269 was applied to the MSS 6 data to produce a normalized image (figure 10). The effectiveness of the non-Lambertian model in reducing the topographic effect was determined by comparing the separability of radiance data for the three dominant slope-aspect classes before and after normalization. Landsat data for three slope-aspect sites were extracted: 1125 pixels for the northwest moderate slope, 231 pixels for northwest steep slope, and 1480 pixels for the southwest moderate slope. The mean values and standard deviations are presented in table 6 and show that the difference in pixel values between the three sites was considerably reduced by the non-Lambertian model. The difference between the mean values for the northwest steep slope and the southeast moderate slope was reduced from 13.9 to 1.9 (86 per cent) in MSS 6 and from 9.7 to 1.2 (87 per cent) in MSS 7. The variation within the sites as measured by the standard deviation increased slightly in the corrected data by an average of 0.5. The results show that the topographic effect was substantially reduced with the non-Lambertian model.

5. Summary of results and conclusion

It is commonly suggested that Landsat cover-classification studies should be undertaken on imagery obtained at high solar elevation to reduce variations in spectral response because of the topographic effect. Results from this study show that even high-sun-angle data have an apparent topographic effect that may confound cover classification. Examination of the June 1976 Landsat imagery showed a marked difference between the radiances associated with the three dominant slope-aspect combinations found in the study area. The topographic effect was evident for MSS 7 and MSS 6 with a pixel-value range of 21 among randomly chosen transects across the study ridge. No topographic effect was apparent in MSS 4 and 5 because of a combination of high absorption in those spectral channels by healthly deciduous vegetation and the Landsat quantization procedure.

Application of four methods for reducing the topographic effect to the sample transects across the test ridge gave the following results:

Spectral-band ratioing (MSS 7/5, MSS 6/5) slightly decreased the variation of the Landsat data for 50 per cent of the transects. Because of the small variation in MSS 5, ratioing could not eliminate the direct-light topographic effect, as the denominator of the ratio was virtually constant. This reasoning also may explain the poor results obtained by Williams *et al.* (1979) with band-ratioing techniques.

When applied to the Landsat data, the Lambertian model increased the topographic effect. This degradation of the radiance is due to the inapplicability of the Lambertian assumption to model the bidirectional reflectance characteristics of the woodland surface.

The modified Lambertian model developed by Civco *et al.* (1977) decreased the variation produced by applying the Lambertian model but gave even higher variances than those found in the raw Landsat data.

The non-Lambertian model developed by Smith *et al.* (1980) markedly decreased (~86 per cent) the variation of the Landsat data, and, therefore, reduced the topographic effect.

Although the non-Lambertian model did not completely eliminate the topographic effect, it considerably reduced the variation. The difference between the mean pixel values associated with the two extreme slope-aspect sites was reduced from 13.9 to 1.9 (86 per cent) in MSS 6 and 9.7 to 1.2 (87 per cent) in MSS 7. The maximum variation between the mean corrected pixel values from the three slope-aspect configurations was 1.9 for MSS 6 and 1.2 for MSS 7.

In conclusion, this study has demonstrated that high-quality digital terrain data such as the USGS DEM data can be used via modelling to enhance the utility of multispectral satellite data. Digital terrain data can be used to develop and test improved radiative transfer models, which, in turn, may lead to improved cover classification of Landsat data.

Although this study has demonstrated the success of a non-Lambertian model for reducing the topographic effect and the potential for preprocessing Landsat data, further development of the existing model is required for application of the technique to more complex surface-cover conditions.

Acknowledgments

The authors thank the USGS Digital Applications Team at Reston, Virginia, particularly Atef Elassal and Frank Beck for providing the DEM data. We also thank Kevin Ingram, CSC, and Ed Masuoka, NASA/GSFC, for their assistance with this project and Anne Heasty, SSA Inc. for the technical editing of this paper.

References

ANUTA, P. E., 1976, *Proc. of 42nd Convention Am. Soc. Photogramm.*, pp. 180-87.

CICONE, R. C., MALILA, W. A., and CRIST, E. P., 1977, *Investigation of techniques for inventorying forested regions. Final Report: Vol. II Forestry information system requirements and joint use of remotely sensed and ancillary data.* NASA-CR-ERIM 122700-35-F2.

CRANE, R. B., 1971, *Proc. of 8th Internat. Symp. of Remote Sensing of Environment*, Ann Arbor, Mich., pp. 1345-1355.

ELASSAL, A., 1980 (personal communication), USGS, Reston.

HOFFER, R. M., and Staff, 1975, *Natural resource mapping in mountainous terrain by computer analysis of ERTS-1 satellite data*, Laboratory for Agricultural Remote Sensing, Purdue, Ind. Information Note 061575.

HOFFER, R. M., FLEMING, M. D., et al., 1979, *Digital processing of Landsat MSS and topographic data to improve capabilities for computerized mapping of forest cover types.* LARS Tech. Rep. 011579.

HOLBEN, B. N., and JUSTICE, C. O., 1979, *Evaluation and modeling of the topographic effect on the spectral response from nadir pointing sensors.* NASA TM 80305, Goddard Space Flight Center, Greenbelt, MD.

HOLBEN, B. N., and JUSTICE, C. O., 1980, *An examination of spectral band ratioing to reduce the topographic effect on remotely sensed data.* NASA TM 80640, Goddard Space Flight Center, Greenbelt, MD.

JUSTICE, C. O., 1978, *Proc. Am. Soc. Photogramm. Fall Mtg.*, Albuquerque, New Mexico, pp. 303-328.

JUSTICE, C. O., and HOLBEN, B. N., 1979, *Examination of Lambertian and non-Lambertian models for simulating the topographic effect on remotely sensed data.* NASA TM 80557, Goddard Space Flight Center, Greenbelt, MD.

JUSTICE, C. O., and HOLBEN, B. N., 1980, *The contribution of the diffuse light component to the topographic effect on remotely sensed data.* NASA TM 85290, Goddard Space Flight Center, Greenbelt, MD.

KRIEBEL, T. K., 1976, *Remote Sensing Environ.* 4, 257-64.

KRIEBEL, T. K., 1978, Appl. Optics 17, 253-259.

KRIEGLER, F. J., MALILA, W. A., NALEPKA, R. F., and RICHARDSON, W., 1969, *Proc. Internat. Symp. on Remote Sen ng of Environ.*, Vol. 1, Ann Arbor, Mich., Oct. 13-16, 1969, pp. 97-109.

MCEWEN, R. B., and ELASSAL, A. A., 1978, *Proc Internat. Users Conf. on Computer Mapping Hardware, Software and Data Bases*, Harvard University, June 1978, p. 23.

MILLER, L. D., NUALCHAWEE, K., and TOM, C., 1978, *Analysis of the dynamics of shifting cultivation in the tropical forests of northern Thailand using landscape modeling and classification of Landsat imagery*. NASA TM 79545, Goddard Space Flight Center, Greenbelt, MD.

MINNAERT, M., 1941, *J. Astrophys.* 93, 403-410.

MINNAERT, M., 1961, in G. P. Kuiper (ed.) *The Solar System, Vol. III, Planets & Satellites*, University of Chicago Press, pp. 213-249.

ROBINSON, N., 1965, *Solar Radiation*. Elsevier Publ. Co., New York.

SADOWSKI, F. G., and MALILA, W. A., 1977, *Investigation of techniques for inventorying forested regions Vol 1 Reflectance modeling & empirical multispectral analysis of forest canopy components*. NAS-CR-ERIM-122700-35-F1.

SHARPNACK, D. A., and AKIN, G., 1969, Photogram. Engng. 3, 247-48.

SMITH, J. A., LIN, T. L., and RANSON, K. J., 1980, The Lambertian assumption and Landsat data. *Photogramm. Engng. Remote Sensing* (in the press).

STOW, D. A., and ESTES, J. E., 1979, *Proc Symp on Machine Processing of Remotely Sensed Data*, Laboratory for Agricultural Remote Sensing, Purdue, Ind., pp. 193-200.

STRAHLER, A. H., LOGAN, T. L., and BRYANT, N. A., 1978, *Proc. 12th Internat. Symp. on Remote Sensing of the Environ*., Manila, Phillippines, Vol. 2., pp. 927-056.

STRAHLER, A. H., LOGAN, T. L., WOODCOCK, C. E., 1979, *Proc. 13th Internat. Symp. on Remote Sensing of Environ.*, Ann Arbor, Michigan, Vol. III, pp. 1541-1555.

TOM, C., MILLER, L. D., and CHRISTENSON, J. W., 1979, *Spatial land use inventory modeling and projection Denver Metropolitan Area with inputs from existing maps, airphotos and Landsat imagery*. NASA TM 79710, Goddard Space Flight Center, Greenbelt, MD.

VINCENT, R. K., 1973, *Proc Am. Soc. Photogramm., Management, Utilization of Remote Sensing Data Conferences*, Sioux Falls, South Dakota, pp. 377-397.

WILLIAMS, D. L. and MILLER, L. D., 1979, *Monitoring forest canopy alteration around the world with digital analysis of Landsat imagery*. Earth Resources Branch, NASA/Goddard Space Flight Center.

WILLIAMS, D. L., STAUFFER, M. L., and LEUNG, K. C., 1979, *Proc. Symp. on Machine Processing of Remotely Sensed Data*, pp. 368-375.

Table 1
Mean, standard deviation, and range of Landsat pixel values for six sample transects across Buffalo Mountain, PA.

Transect	Multispectral scanner	Pixel Value			N
		Mean	Standard deviation	Range	
1	4	16.1	0.64	2	20
	5	12.6	0.68	2	
	6	60.0	4.9	16	
	7	34.2	3.2	9	
2	4	16.0	0.83	3	20
	5	12.6	0.60	2	
	6	59.0	4.8	15	
	7	33.5	3.7	13	
3	4	16.2	0.64	2	20
	5	12.3	0.73	2	
	6	60.9	6.0	21	
	7	34.5	3.7	13	
4	4	15.9	0.72	2	20
	5	12.5	0.60	2	
	6	59.3	4.6	15	
	7	33.7	2.5	8	
5	4	15.8	0.87	3	20
	5	12.6	0.74	2	
	6	59.5	4.4	14	
	7	34.0	3.1	12	
6	4	15.9	0.82	3	20
	5	12.7	0.79	3	
	6	61.6	6.5	18	
	7	35.0	5.3	14	

Table 2
Pearson's product-moment correlation coefficients (r) for Landsat radiances and data derived from the radiance models for six transects.

Transect no.	Multispectral scanner	N	Model†		
			1	2	3
1	4	20	−0.39*	−0.27*	0.20*
	5		0.13*	−0.08*	0.01*
	6		0.88	−0.84	−0.85
	7		0.89	−0.88	0.88
2	4	20	−0.07*	−0.02*	0.30*
	5		0.26*	−0.11*	−0.11*
	6		0.90	−0.93	0.89
	7		0.89	−0.87	0.87
3	4	20	0.57*	−0.57*	0.40*
	5		0.54*	−0.49*	0.40*
	6		0.93	−0.84	0.91
	7		0.91	−0.79	0.90
4	4	20	−0.20*	0.28*	0.24*
	5		0.57*	−0.52*	0.44*
	6		0.96	−0.90	0.96
	7		0.97	−0.94	0.96
5	4	20	0.24*	−0.29*	0.43*
	5		−0.28*	−0.28*	0.08*
	6		0.84	−0.66	0.85
	7		0.89	−0.78	0.89
6	4	20	0.27*	−0.32*	0.24*
	5		0.27*	−0.39*	0.27*
	6		0.94	−0.94	0.94
	7		0.97	−0.95	0.96

† Model 1 Cosine i
2 Modified cosine i
3 Non-Lambertian model
* Insignificant at the 0.05 level of probability.

Table 3
Coefficients of variation for the uncorrected and corrected transect data.

Transect no.	Multispectral scanner channel	Coefficient of variation (per cent)				Ratio 6/5	Ratio 7/5
		Uncorrected Landsat	Lambertian model	Modified Lambertian model	Non-Lambertian model		
1	4	4.0	31.5	8.1	–	9.1	11.2
	5	5.4	30.5	10.0	–		
	6	8.1	22.9	15.3	4.3		
	7	9.5	21.7	16.8	4.6		
2	4	5.1	42.1	10.3	–	8.5	10.6
	5	4.7	38.1	10.2	–		
	6	8.2	32.6	16.5	3.8		
	7	11.1	27.7	18.6	5.5		
3	4	3.9	21.0	11.9	–	7.2	8.5
	5	6.0	29.5	13.2	–		
	6	9.9	22.7	18.1	4.2		
	7	10.7	21.6	18.5	4.9		
4	4	4.5	37.2	7.6	–	6.6	6.0
	5	4.8	30.8	10.6	–		
	6	7.7	26.6	14.6	2.2		
	7	7.5	26.4	14.5	2.1		
5	4	5.5	40.4	10.2	–	9.9	12.2
	5	5.9	41.1	7.9	–		
	6	7.5	32.6	13.2	4.0		
	7	9.1	29.4	15.2	4.2		
6	4	5.2	43.5	11.3	–	9.8	14.0
	5	6.2	43.9	12.3	–		
	6	10.5	34.4	18.5	3.9		
	7	15.0	28.2	22.7	4.0		

Table 4

Minnaert K values and coefficients of determination (r^2) for the six sample transects.

Transect	Multispectral scanner channel	N	K	r^2
1	4	20	−0.04	0.07
	5		0.03	0.03
	6		0.26	0.76
	7		0.30	0.80
2	4	20	0.01	0.00
	5		0.07	0.16
	6		0.22	0.83
	7		0.32	0.82
3	4	20	0.09	0.34
	5		0.13	0.34
	6		0.32	0.85
	7		0.35	0.84
4	4	20	0.01	0.01
	5		0.14	0.50
	6		0.27	0.94
	7		0.27	0.95
5	4	20	0.05	0.10
	5		−0.02	0.01
	6		0.20	0.74
	7		0.26	0.82
6	4	20	0.05	0.13
	5		0.05	0.10
	6		0.25	0.89
	7		0.37	0.94

Table 5

Coefficients of variation (CV) for the non-Lambertian model applied to the sample transects, substituting a range of Minneart K values.

Transect no.	Multispectral scanner channel	CV (per cent) with indicated K values											CV of raw data
		0	0.1	0.2	0.3	0.4	0.5	0.6	0.7	0.8	0.9	1.0	
1	6	8.5	6.2	4.6	4.4	5.9	8.3	10.9	13.8	16.8	19.8	22.9	8.1
	7	9.7	7.3	5.4	4.6	5.5	7.5	10.0	12.8	15.7	18.7	21.7	9.5
2	6	8.8	5.8	3.9	4.7	7.7	11.3	15.2	19.3	23.5	28.0	32.6	8.2
	7	12.2	9.4	6.9	5.6	6.3	8.7	11.9	15.5	19.4	23.5	27.2	11.1
3	6	10.3	7.8	5.6	4.3	4.9	7.0	9.8	12.8	16.0	19.3	22.7	9.8
	7	11.3	8.8	6.6	5.1	5.2	6.8	9.2	12.1	15.1	18.3	21.6	10.7
4	6	8.9	5.9	3.2	2.5	4.9	8.2	11.7	15.3	19.0	27.7	26.6	7.7
	7	8.8	5.8	3.0	2.3	4.9	8.1	11.6	15.1	18.8	22.5	26.3	7.5
5	6	7.7	5.1	4.0	5.5	8.5	12.0	15.7	19.7	23.8	28.1	32.6	7.5
	7	9.6	6.8	4.7	4.4	6.5	9.7	13.2	17.0	21.0	25.1	29.4	9.1
6	6	10.8	7.2	4.4	4.5	7.6	11.6	15.9	20.4	25.0	29.7	34.4	10.5
	7	15.4	11.8	8.2	5.1	4.1	6.6	10.4	14.6	19.0	23.5	28.1	15.0

Table 6

Mean pixel values and standard deviations calculated for uncorrected data and data corrected with the non-Lambertian model for three slope-aspect sites.

Slope-aspect site	Mean incidence angle	N	Pixel value							
			Uncorrected data				Corrected			
			MSS 6		MSS 7		MSS 6		MSS 7	
			$\bar{x}$	SD	$\bar{x}$	SD	$\bar{x}$	SD	$\bar{x}$	SD
Northwest (moderate slope)	62°	1125	56.3	3.3	31.9	2.1	68.4	4.1	40.0	2.6
Northwest (steep slope)	40°	231	50.7	2.2	27.8	1.3	67.0	2.9	39.7	1.8
Southeast (moderate slope)	72°	1480	64.6	2.6	37.6	1.7	68.9	2.9	40.9	1.8
Maximum range in means			13.9		9.7		1.9		1.2	

List of Figures

Figure 1. Location of the study area (rectangle) on Landsat MSS image December 1973, solar elevation 21

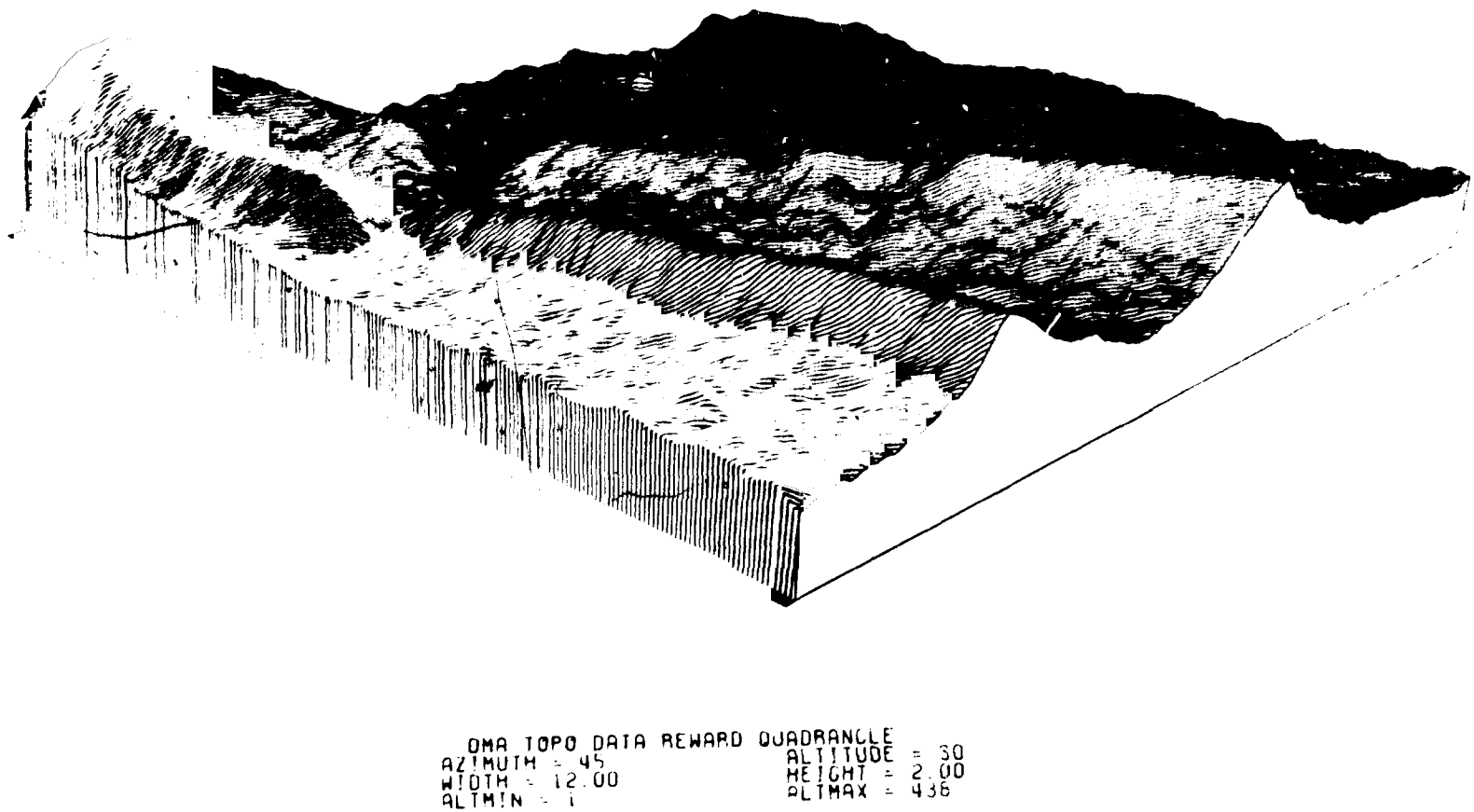

Figure 2. Block diagram of the Reward Quadrangle from the southeast, constructed with digital terrain data.

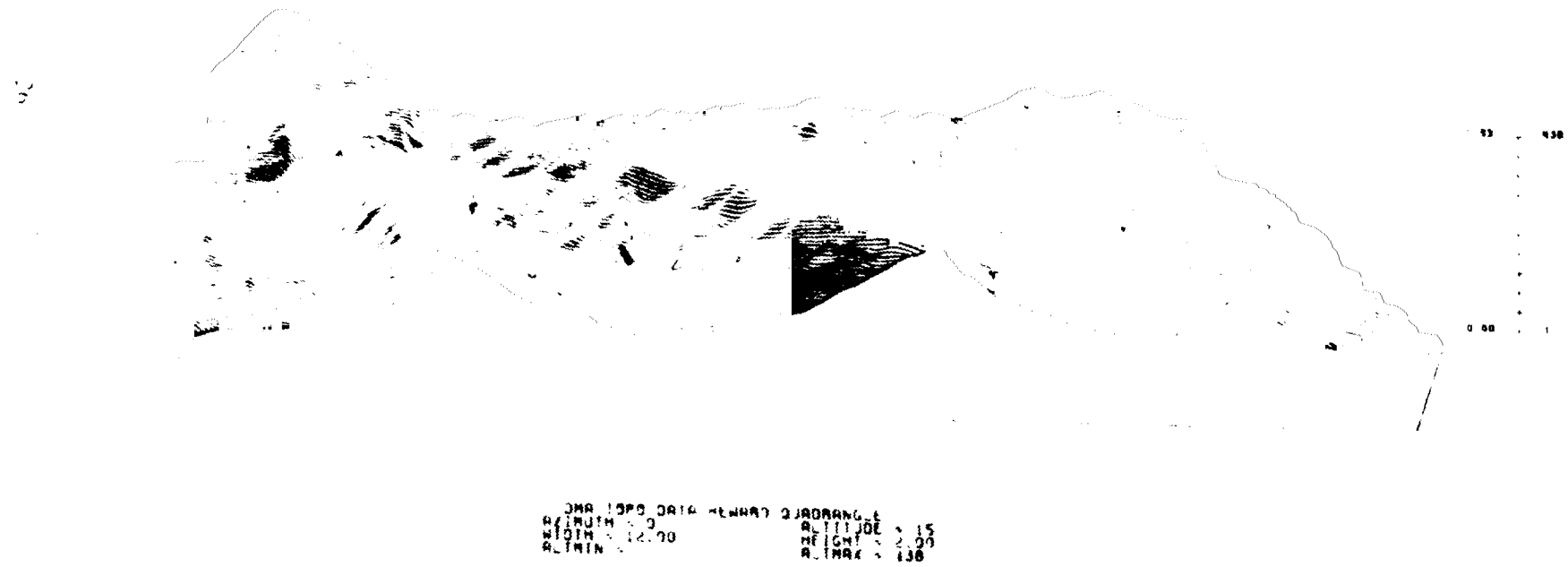

Figure 3. Block diagram of the Reward Quadrangle from the East, constructed with digital terrain data.

Figure 4. Digital elevation model data of the Reward Quadrangle (dark areas represent low elevation, light areas represent high elevation)

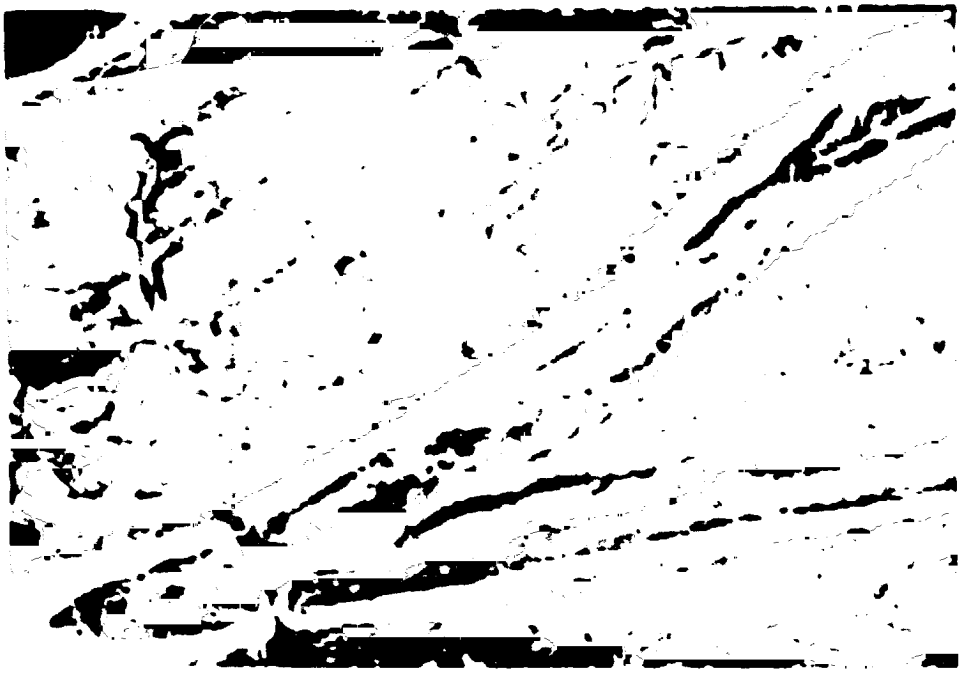

Figure 5a. Slope-angle map of the Reward Quadrangle created from digital elevation data (Dark areas represent low slopes, light areas represent high slopes)

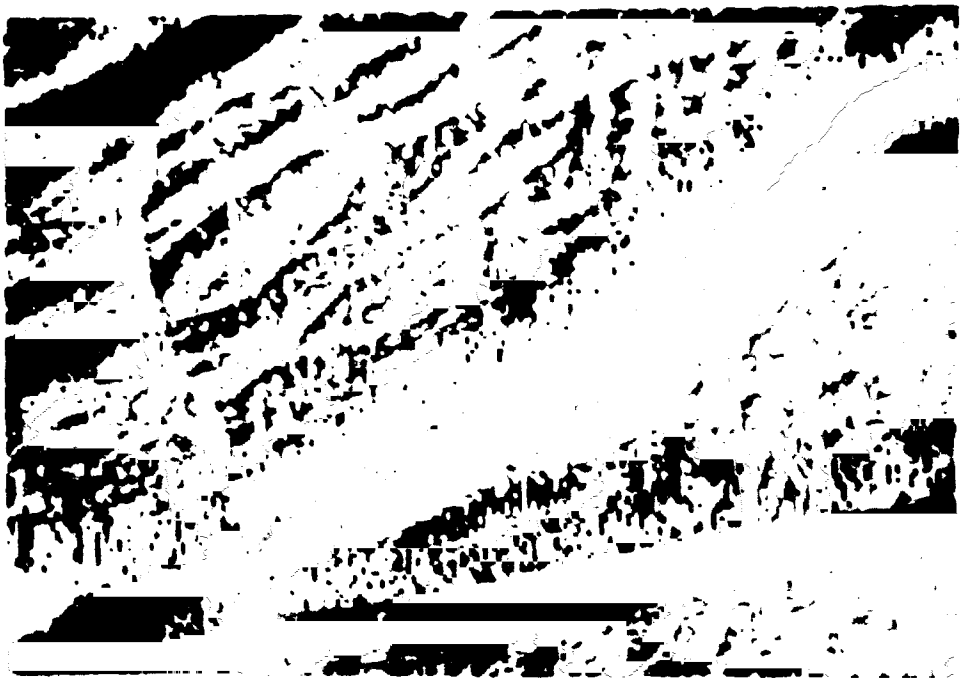

Figure 5b. Slope aspect map of the Reward Quadrangle created from digital elevation data. (lightest tone = 0°, darkest tone = 359°).

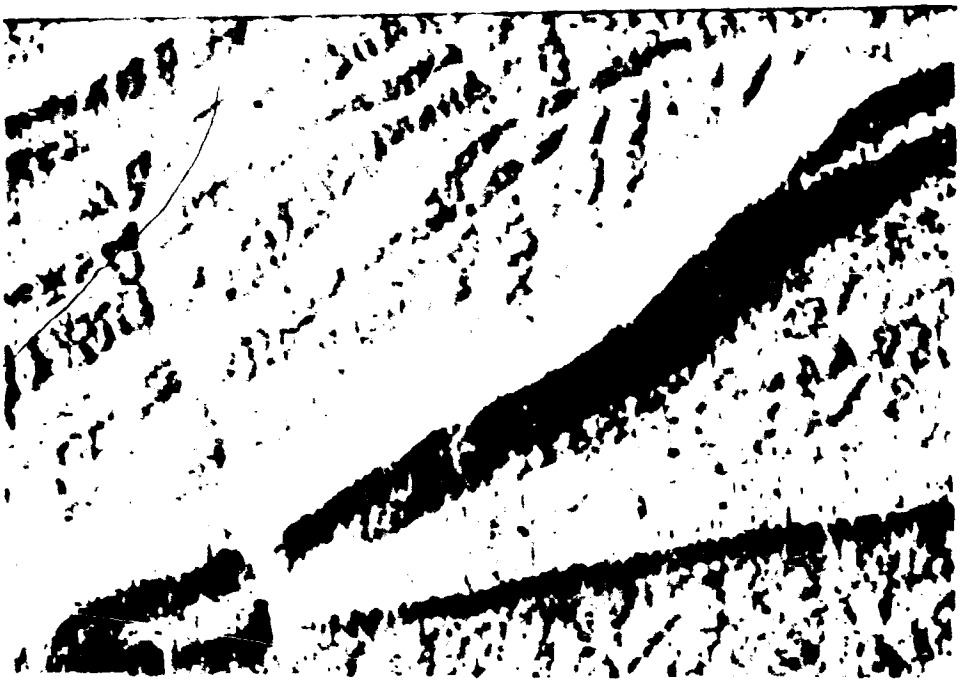

Figure 5c. Incidence angle of the Reward Quadrangle for 55° solar elevation. (dark tones represent low incidence angles, light tones represent high incidence angles).

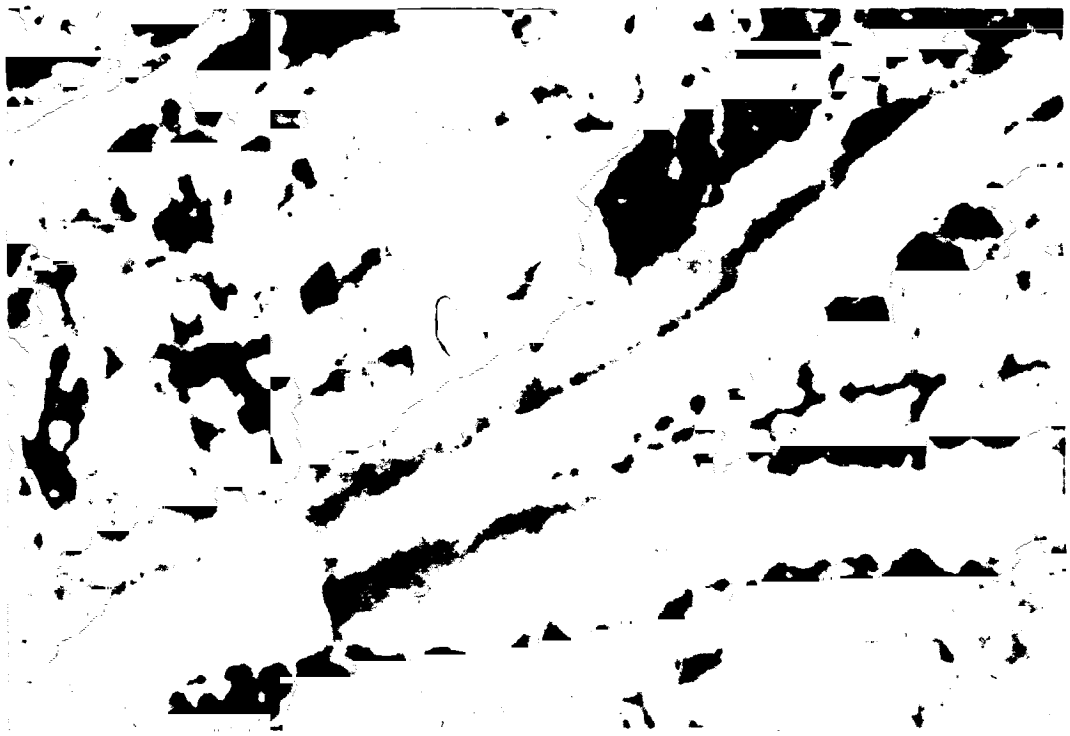

Figure 6. Landsat MSS 7 of the Reward Quadrangle.

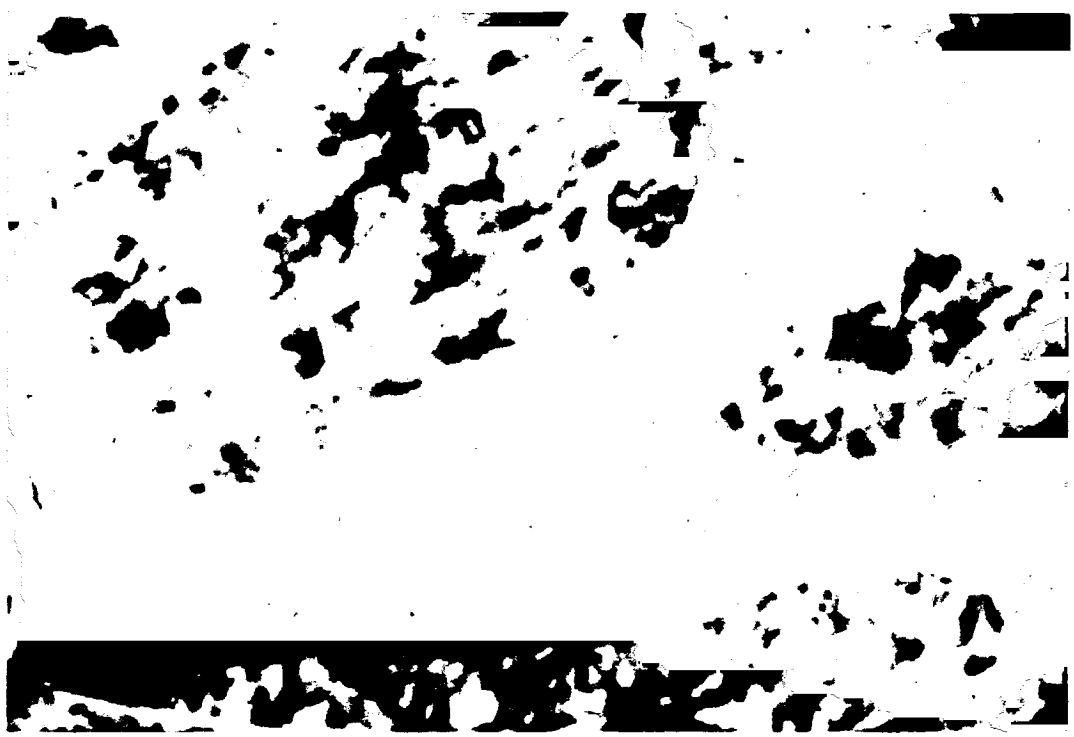

Figure 7. Landsat MSS 5 of the Reward Quadrangle.

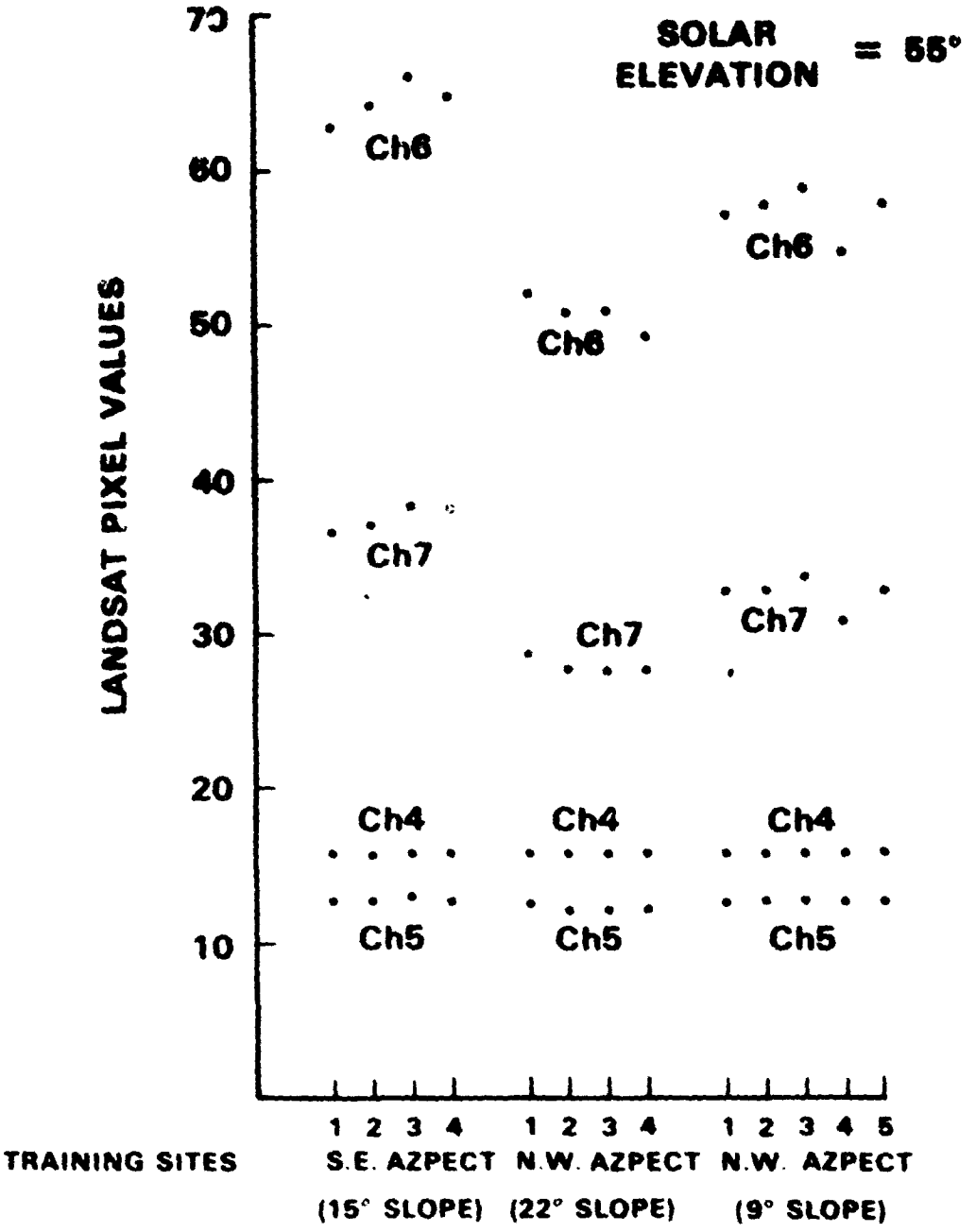

Figure 8. Plot showing the distribution of mean Landsat pixel values associated with the training sites from different slopes and aspects.

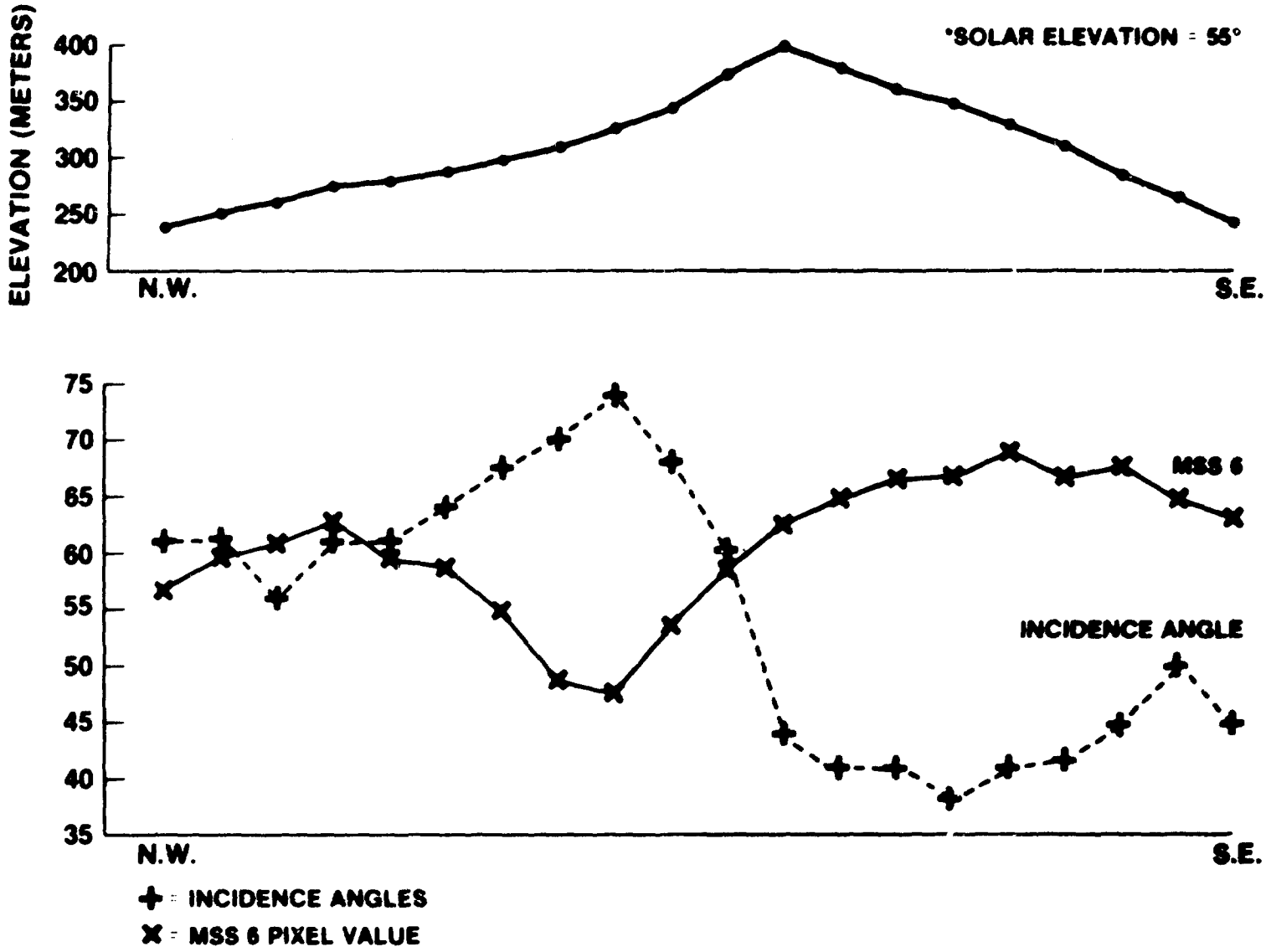

Figure 9. Elevation, incidence angles, and Landsat multispectral scanner 6 response for a sample transect across Buffalo Mountain.

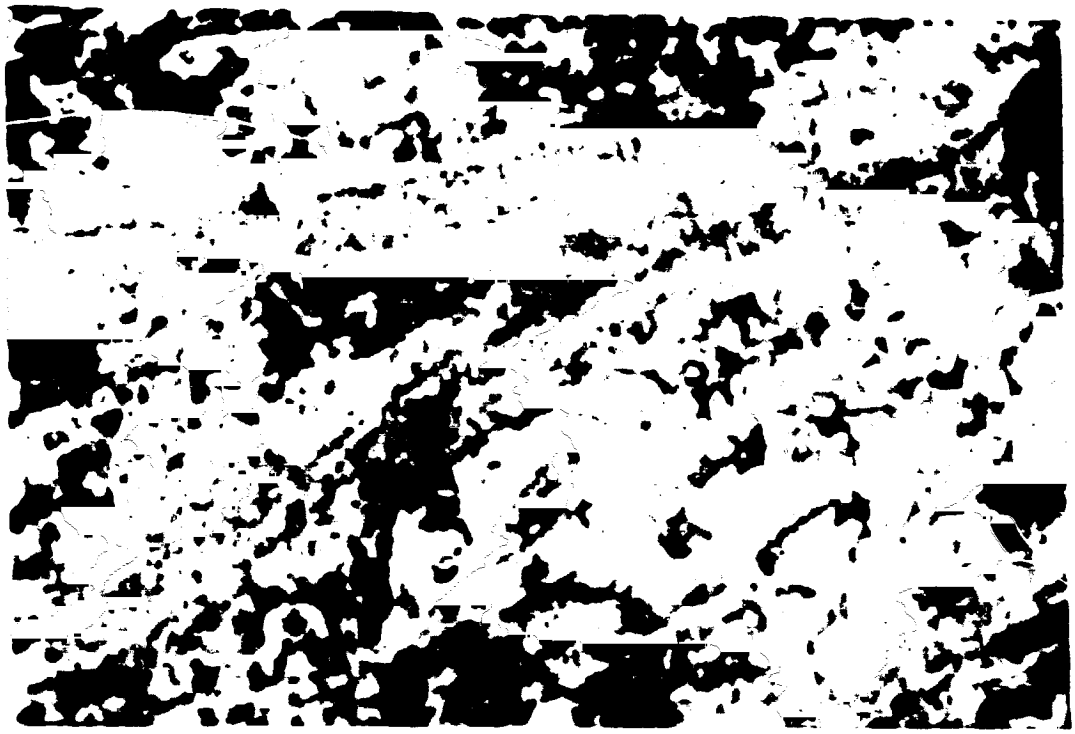

Figure 16. MSS 6 data normalized with the non-Lambertian model.

END

DATE

FILMED

FEB 10 1981